Rapid Communications

Excited states of neutral and charged excitons in single strongly asymmetric InP-based nanostructures emitting in the telecom C band

M. Gawełczyk,[1,2,*] P. Wyborski,[2] P. Podemski,[2] J. P. Reithmaier,[3] S. Höfling,[4,5] and G. Sęk[2]

[1]*Department of Theoretical Physics, Wrocław University of Science and Technology, PL-50-370 Wrocław, Poland*

[2]*Laboratory for Optical Spectroscopy of Nanostructures, Department of Experimental Physics, Wrocław University of Science and Technology, PL-50-370 Wrocław, Poland*

[3]*Institute of Nanostructure Technologies and Analytics (INA), CINSaT, University of Kassel, Heinrich-Plett-Strasse 40, D-34132 Kassel, Germany*

[4]*Technische Physik, University of Würzburg and Wilhelm-Conrad-Röntgen-Research Center for Complex Material Systems, Am Hubland, D-97074 Würzburg, Germany*

[5]*SUPA, School of Physics and Astronomy, University of St. Andrews, North Haugh, St. Andrews KY16 9SS, United Kingdom*

(Received 25 July 2019; revised manuscript received 16 October 2019; published 27 December 2019)

We investigate strongly asymmetric self-assembled nanostructures with one of the dimensions reaching hundreds of nanometers. Close to the nanowirelike type of confinement, such objects are sometimes assigned as one dimensional in nature. Here, we directly observe the spectrum of exciton excited states corresponding to longitudinal quantization. This is based on probing the optical transitions via polarization-resolved microphotoluminescence excitation (μPLE) measurements performed on single nanostructures combined with theoretical calculations of the neutral and charged exciton optical properties. We successfully probe absorptionlike spectra for individual bright states forming the exciton ground-state fine structure, as well as for the negatively charged exciton. Confronting the calculated spectrum of excitonic absorption with μPLE traces, we identify optical transitions involving states that contain carriers at various excited levels related to the longest dimension. Based on a cross-polarized excitation-detection scheme, we show a very well-conserved spin configuration during orbital relaxation of the exciton from a number of excited states comparable to the quasiresonant pumping via the optical phonon, and no polarization memory for the trion, as theoretically expected.

DOI: 10.1103/PhysRevB.100.241304

Out of the variety of semiconductor nanostructures, those prepared via molecular beam epitaxy (MBE) in InAs on InP-substrate systems [1], especially InAs/AlGaInAs considered here [2], typically stand out with a high areal density and an in-plane elongation so high that it is disputable whether they should be classified as quantum dots (QDs) or quantum wires [3–6]. This fundamental ambiguity did not prevent the intense research on the properties of such objects. They have been studied both as ensembles [3,7–9] and single objects [10–13] showing the potential for implementation in optoelectronics such as telecom lasers and optical amplifiers [8,14–16] or single-photon sources for fiber networks [12,17]. Notably, their emission energy is tuned deterministically over the telecom C band with the amount of deposited InAs [2].

Several other strategies for achieving telecom emission from epitaxial QDs have been actively developed, including sophisticated approaches such as deposition on metamorphic buffers or droplet epitaxy. These proved successful on both GaAs and InP substrates [18–21] and yielded low or vanishing exciton fine-structure splitting (FSS). In parallel, efforts aiming at improving the properties of self-assembled MBE-grown InP-based nanostructures such as those considered here continue. Cancellation of FSS is achievable also in this case via an approach proposed earlier [22].

Regarding basic research, recent studies brought an understanding of the exciton ground-state (GS) properties in investigated QDs including partially polarized emission [23] and two-exponential recombination [6], and raised questions about the exciton confinement regime [24,25]. Although excited exciton states in QDs were the subject of a recent deep study [26], the realm of highly elongated dots remains weakly covered in this context, with a single work for InAs/InP QDs [27], where, however, the confinement is different. The available QD-ensemble absorption data [28,29] are insufficient, as energy separations below the ensemble bandwidth are expected for quantization in the longest dimension [6]. Thus, high-resolution photoluminescence excitation [microphotoluminescence excitation (μPLE)] spectroscopy measurements are needed. These are widely used for QDs emitting below 1 μm, but are experimentally challenging in the telecom range. One remedy is to use pulsed excitation [30]. This, however, provides a low average power and can increase the linewidth, which obstructs the resolution of individual transitions, whose ladder is dense for investigated QDs.

Here, we use an experimental setup built for μPLE studies of single nanostructures emitting in the infrared [31], especially in the third telecom window. We successfully probe the spectrum of optically active excited states of C-band-emitting

*michal.gawelczyk@pwr.edu.pl

QDs elongated above 100 nm, including individual bright states forming the exciton fine structure, and the negatively charged exciton (X^-). Confrontation of these μPLE data with calculated absorption spectra indicates the presence of states that involve electron and hole excitations related to the longest QD dimension. With this, we unambiguously confirm the zero-dimensional nature of the studied objects, i.e., energy quantization in all spatial dimensions. While additional localization in quantum wires is known to lead to energy quantization [32], here we demonstrate quantization in the longest QD dimension exceeding 100 nm, although no further effective size reduction occurs. The agreement of simulated and experimental spectra allows us to label the transitions with electron-hole orbital-state configurations forming respective excited states. These are dominated by highly excited hole state contributions due to weak hole confinement in the system. Additionally, in a polarization-resolved excitation-detection scheme, we observe a mostly conserved spin configuration during orbital relaxation from a number of states for the neutral exciton and, contrarily, no spin memory for X^-, in agreement with theoretical considerations.

The investigated sample was grown by gas-source MBE on an InP:S substrate [2]. Deposition of 1.26 nm of InAs onto a 200-nm-thick $Al_{0.24}Ga_{0.23}In_{0.53}As$ barrier layer yielded a Stranski-Krastanov formation of nanostructures on a wetting layer (WL) that were then covered with a 100-nm-thick barrier layer and 20 nm of InP. Imaging of the uncapped sample showed a dense ($>10^{10}$ cm^{-2}) ensemble of nanostructures strongly elongated in the $v \equiv [1\bar{1}0]$ direction ($h \equiv [110]$). Their cross sections are trianglelike with a width-to-height ratio of $W/H \approx 6$ [2]. The length L may significantly exceed 100 nm [23,29], which places the structures on a crossover between dot- and wirelike confinements. To enable optical experiments on single nanostructures, the sample was processed by electron beam lithography and etching, which left submicrometer mesas.

During experiments the sample was kept in a continuous-flow liquid-helium cryostat at $T = 4.2$ K. Structures were excited either nonresonantly with a continuous-wave (cw) 639-nm laser line, or quasiresonantly with an external-cavity cw laser in the Littrow configuration with a tuning range of 1440–1540 nm. The excitation beam was filtered with a shortpass filter and a 300-mm-focal-length monochromator to improve its quality. A spatial resolution of ~2 μm was obtained by passing both the excitation beam and the collected signal through a microscope objective with 0.4 numerical aperture. After removing the scattered laser line with a long-pass or bandpass filter, the collected signal was guided to an analyzer consisting of a 1-m-focal-length monochromator and a GaInAs-based multichannel detector providing a total spectral resolution of ~50 μeV. Rotation of a half-wave plate in front of a linear polarizer allowed for polarization control in both excitation and collection.

In Fig. 1(a), we plot microphotoluminescence (μPL) spectra collected from a selected 550×275 nm$^2 \approx 0.15$ μm^2 mesa at various power densities P of nonresonant cw excitation ($P_0 \sim 30$ nW/μm^2 in the spot). Those from observed well-resolved lines covering the C band that occur already at the lowest power come from carrier-complex GSs. We choose three marked with arrows (A–C) for further analysis, based on

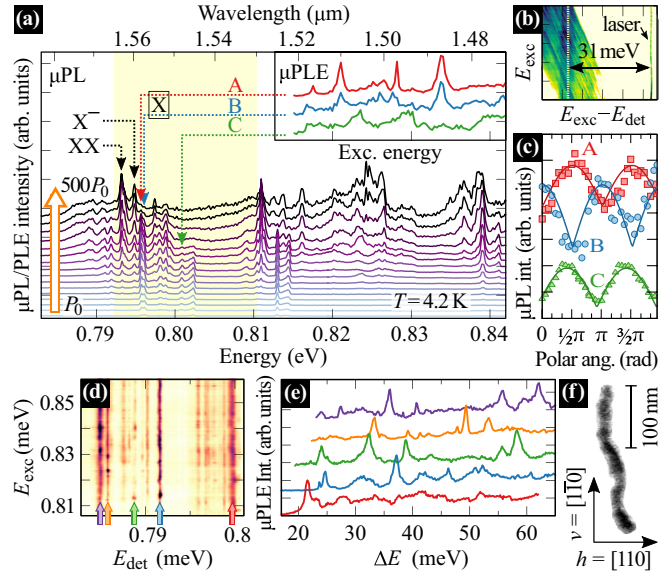

FIG. 1. (a) Power series of μPL spectra. Inset: μPLE collected at energies marked with arrows (A–C); the energy axis is common. (b) Photoluminescence excitation map from an ensemble of QDs; the LO-phonon line marked. (c) Polarization-resolved μPL with $a\,|\sin x|$ fits for lines A–C. (d) μPLE color map for an exemplary mesa with QDs. (e) μPLE spectra collected at energies marked on the map. (f) Single QD top view extracted from a scanning electron microscopy image of an uncapped sample.

their linear growth with excitation power. The polarization-resolved μPL shows no fine-structure splitting within the available resolution for line C, which thus comes most probably from X^-, as the positively charged exciton is less probable to be formed in this system [27,33]. Studied QDs, due to their asymmetry, show FSS in the range of 50–180 μeV [33], so our spectral resolution along with the polarization properties of the line allow for this assignment. Contrarily, lines A and B come from two spin configurations of the same exciton GS with FSS $\simeq 240$ μeV, which exceeds previous observations [27,33]. In Fig. 1(c), we show intensities of these lines versus polarization angles relative to [110], where A and B are in antiphase, as expected. See Supplemental Material [34] for a more detailed analysis of the A-B-XX recombination cascade.

Additionally, in the inset to Fig. 1(a), μPLE spectra collected at energies corresponding to chosen emission lines are shown. Noticeably, traces for A and B are similar, which confirms their classification. To support the analysis, we show in Fig. 1(b) a QD-ensemble photoluminescence excitation map, with a line occurring at a fixed ~31 meV separation from the laser, identified as the longitudinal optic (LO)-phonon-assisted absorption [38]. Apparently, the volume of QDs is large enough to modify phonon dispersion, as the LO-phonon energy in AlGaInAs is $E_{LO} \sim 36$ meV, and the one observed is closer to the InAs value.

Next, in Fig. 1(d), we present a typical excitation-detection map, where each vertical cross section forms a μPLE spectrum. Arrows mark the lines, the spectra for which are plotted in Fig. 1(e). Their significant diversity reflects the inhomogeneity of QDs in question: Spread lengths, and factors such as local widenings and bends visible in Fig. 1(f). Note that the

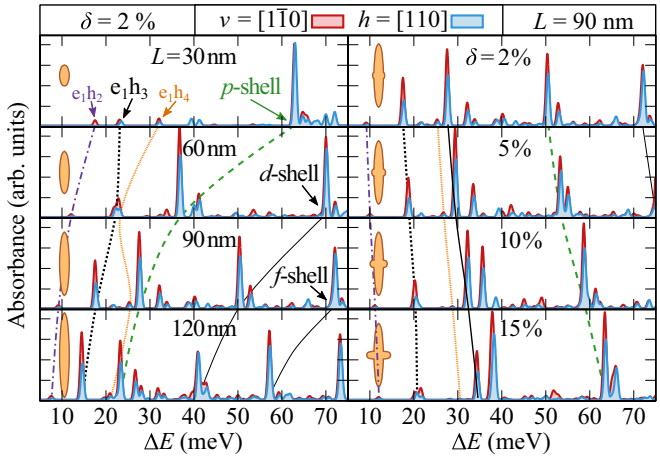

FIG. 2. Calculated polarization-resolved neutral-exciton absorption spectra for various QD lengths L (left) and hump sizes δ (right). Insets: Schematic QD geometry.

height of the PLE peaks results from both the absorption rate and effective orbital relaxation rate for the given ΔE.

To understand the μPLE data, we calculate the optical properties of excited states for QDs of various geometries. Protruding from a 0.9-nm-thick WL, modeled QDs have a triangular cross section, $W/H = 6$, and an elliptical longitudinal height profile. To account for material intermixing, we perform Gaussian averaging with $\sigma = 0.9$ nm [6]. Apart from varying H in the range of 1.8–3.3 nm and L within 30–280 nm, we account for the expected perturbed geometry [see Fig. 1(f) and Ref. [23]] via a 10-nm-long central hump with a $(1+\delta)$ times enlarged cross section (see the insets in Fig. 2). Conduction- and valence-band electron states are calculated using the eight-band envelope-function $\boldsymbol{k}\cdot\boldsymbol{p}$ theory [39–41]. We use a numerical implementation [42] that includes spin-orbit effects, strain, and a nonlinear piezoelectric field (for details and parameters, see Ref. [6]). Then, we construct carrier-complex states via diagonalization of the Coulomb and anisotropic electron-hole exchange interactions within the configuration-interaction approach (46 × 46 single-particle configurations used) and calculate polarization-resolved oscillator strengths in the dipole approximation [43]. To simulate the absorption spectra, we widen each line by $\Delta E = \hbar/\tau$ (τ is the calculated lifetime), and convolute with a Gaussian (and its LO-phonon replicas) of $\sigma = 0.2$ meV to represent the laser linewidth, spectral diffusion, and phonon effects [44]. Where compared with experiment, curves are scaled with $1-\exp(-ax)$ to account for state saturation.

Calculated absorption spectra are plotted in Fig. 2. While H determines the GS energy E_0, it weakly affects the relative positions of the states, thus we present only results for $H =$ 3.3 nm corresponding to $E_X \sim 0.8$ eV: For QDs with $\delta = 2\%$ and varying $L = 30$–120 nm (left), and for fixed $L = 90$ nm with varied δ (right). The two curves represent absorption of v/h-polarized light. Phonon replicas are disabled here for clarity. Understandably, with rising L the spectrum gets denser. The hump reduces E_0, thus shifting the excited states to higher relative energies without much change in their spacing. The dashed line traces the p-shell redshift following a $\sim 1/L$

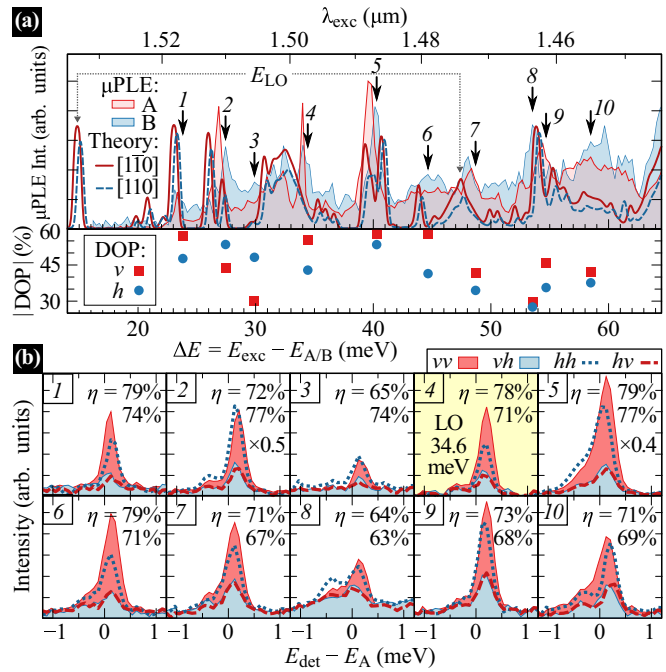

FIG. 3. (a) μPLE spectra for the exciton fine-structure pair of lines [A and B in Fig. 1(a)] (solid) and calculated polarization-resolved absorption spectra for QD with $L = 140$ nm, $\delta = 5\%$ (lines); absolute values of DOP for emission under v- and h-polarized excitation at marked peaks (symbols, bottom panel). (b) μPL of given lines for excitation at marked μPLE maxima in various configurations of excitation-detection polarization.

trend that has been already noticed [6]. Additionally, another significantly bright state emerges with the increase of QD length below the p shell. It is predominantly composed of the GS electron and the hole at the third orbital level (three antinodes along the QD). The high confinement anisotropy results in nearly independent subladders of excitations in the in-plane directions with level spacings defined by L and H [6]. Effectively heavier holes experience shallow confinement in this material system, hence the spacing of their longitudinal excitations is on the level of single meV's. This underlies the presence of the bright state below the p shell. We additionally trace higher shells and two nominally dark states e_1h_2, e_1h_4. All states have two bright spin configurations coupling to v- and h-polarized light.

Returning to lines A and B from Fig. 1(a), in Fig. 3(a) we confront their μPLE traces with calculated absorption spectra. Judging by the agreement, the line likely comes from a QD well modeled by $L = 140$ nm and $\delta = 5\%$. Here, we set $E_{\mathrm{LO}} = 32.5$ meV, based on visible wide phonon replicas. The one sharp line at ∼34 meV without a counterpart in theory is likely a bulk phonon replica, as opposed to wide peaks originating from perturbed phonon modes. While the calculated position of the e_1h_3 state is below the range of experimental data, its replica fits well the widened experimental peak at $\Delta E \simeq 48$ meV, which, according to calculation, is formed by overlapping the e_1h_3 replica and another transition. We characterize also other excited states corresponding to marked peaks, as presented in Table I via a few dominant single-particle contributions. We label them

TABLE I. Calculated energy, oscillator strengths $f_{v/h}$, and single-particle components of exciton states (contribution size indicated by color intensity) matching selected transitions in Fig. 3.

ΔE_{exp} (meV)	23.8	27.4	29.9	40.3	44.7	48.9	53.5	54.7	58.5
ΔE_{calc} (meV)	23.1	27.2	29.5	40.6	43.9	47.4	53.9	55.1	58.1
f_v	6.5	1.1	0.083	3.8	0.67	0.25	2.9	0.59	0.21
f_h	4.0	0.70	0.064	3.3	0.39	0.20	2.6	0.35	0.20
e states contribution $n{:}\,n_v\,\vert\,n_h$	1: 1|1	1: 1|1	1: 1|1	1: 1|1	1: 1|1	1: 1|1	1: 1|1	1: 1|1	1: 1|1
	2: 2|1	2: 2|1	2: 2|1	2: 2|1	2: 2|1	2: 2|1	3: 3|1	3: 3|1	3: 3|1
	3: 3|1	3: 3|1		3: 3|1	3: 3|1	3: 3|1	4: 4|1	2: 2|1	4: 4|1
				4: 4|1		4: 4|1	2: 2|1	4: 4|1	2: 2|1
h states contribution $n{:}\,n_v\,\vert\,n_h$	2: 2|1	4: 4|1	9: 2|2	7: 6|1	12: 9|1	19: 2|3	4: 4|1	8: 7|1	23: 13|1
	3: 3|1	3: 3|1	6: 1|2	12: 9|1	5: 5|1	5: 5|1	20: 12|1	20: 12|1	5: 5|1
	1: 1|1	2: 2|1	13: 4|2	3: 3|1	9: 2|2	7: 6|1	22: 3|3	12: 9|1	7: 6|1
		1: 1|1		4: 4|1	7: 6|1	2: 2|1	5: 5|1	10: 8|1	8: 7|1
				5: 5|1	10: 8|1	14: 10|1	7: 6|1	7: 6|1	12: 9|1

by the state number n and axiswise excitations $n_{v/h}$, i.e., numbers of antinodes along v and h. Noticeably, no purely p-shell state is present, as it got mixed with e_1h_3 (first column). While all states are predominantly composed of the GS electron configurations with weaker admixtures of few excited levels, the hole contributes significantly with a number of excited states: Both subladders of states are involved, with the dominance of longitudinal excitations. An analogous discrete absorption spectrum could not be obtained assuming the quantum-wire confinement limit. For more examples of theoretically reproduced μPLE spectra, see Supplemental Material [34].

Inefficient spin relaxation in QDs should allow for the preservation of linear polarization between pumping into an excited exciton state and GS emission. To verify this, we present in Fig. 3(b) the μPL from lines A and B in four configurations of excitation-detection linear polarization and under pumping into selected μPLE peaks. The highlighted panel corresponds to the peak identified as an overlap of LO-phonon-assisted GS and excited-state absorption. Based on the expected high efficiency of the former, which should be spin preserving, we use the corresponding values of the polarization-injection efficiency $\eta_{v/h} = I_{v/h}/(I_{v/h} + I_{h/v})$ as a reference. These are equal $\eta_v^{(\mathrm{LO})} = 78\%$, $\eta_h^{(\mathrm{LO})} = 71\%$ and do not stand out from those obtained for other lines. Thus, exciton relaxation through the ladder of states in the probed range of energies is highly spin preserving. While higher than those obtained earlier for quasiresonant pumping of a QD ensemble [45], the values of η presented here are subideal, partly due to the unavoidable misalignment of misshapen QDs with respect to the polarization axes. In Fig. 3(a) we replot these data in the form of a v-axis degree of polarization, $\mathrm{DOP} = (I_v - I_h)/(I_v + I_h)$, of emission under excitation with each of the polarizations (note that for h-pumping $\mathrm{DOP} < 0$, and we show $|\mathrm{DOP}|$).

Next, we repeat the analysis as above for the X^- line from another mesa. In Fig. 4(a), we plot the corresponding μPLE trace with an agreeing calculated absorption spectrum, achieved for $L = 140$ nm, $\delta = 10\%$. Notably, the low-energy states predicted by calculation below the experimental range have phonon replicas in the measured μPLE signal. Apart from a denser state ladder due to the three-particle nature of the complex, the main difference relative to the exciton is the absence of a fine structure and the resultant linear polarization

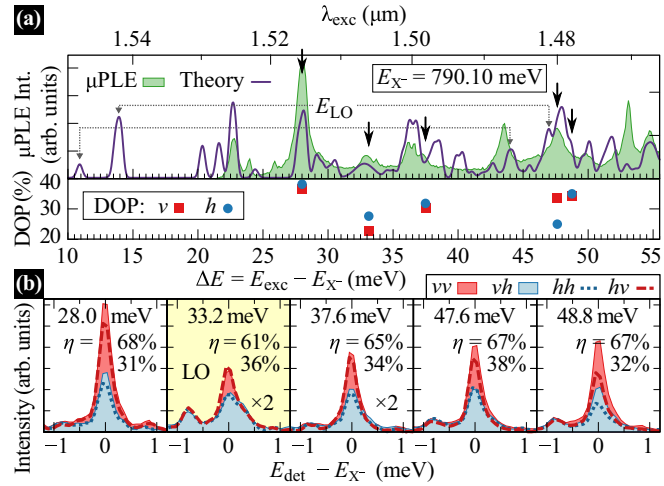

FIG. 4. As in Fig. 3 but for X^-, $L = 140$ nm, $\delta = 10\%$.

of absorbed light. Here, bright spin configurations couple to light polarized elliptically, with major axes inclined towards v for both states. Consequently, the two states should get equally occupied under both pumping polarizations, and emit with an elliptical one, with linear projections equally unequal for both states. This is revealed in polarization-resolved μPL from the given line under polarized excitation presented in Fig. 4(b), where approximately no impact of pumping beam polarization on the emission is observed, and reflected in DOP plotted in Fig. 4(a). The values of η_v are misleading here, as the states naturally emit partly polarized light. Thus, as the elliptical basis is nonorthogonal, polarized light cannot be used to selectively address the X^- states.

In conclusion, we have studied the spectrum of optically active excited states in QDs of an InP-based material system characterized by strong in-plane anisotropy and emitting in the telecom C band. We have used an experimental setup with filtered tunable external-cavity laser excitation providing a high spatial resolution and tuned excitation in the infrared. Performing μPLE experiments on single QDs, we have obtained absorptionlike spectra of neutral and charged excitons. Combining this with calculations, and based on the agreement, we have identified transitions involving states that contain carriers at various excitation levels related to the longest QD dimension. This confirms the zero-dimensional character of carrier confinement in the studied QDs, which are often treated and modeled as one-dimensional quantum wires. Additionally, using a cross-polarized excitation-detection scheme, we have shown highly spin-preserving exciton relaxation in a range of excitation energies. Contrarily, but in line with theory, the charged exciton showed no such linear-polarization memory.

We acknowledge support from the National Science Centre (Poland) under Grants No. 2014/14/M/ST3/00821 and No. 2014/15/D/ST3/00813. The project has also been financially supported by the Polish National Agency for Academic Exchange. P.W. acknowledges support by the European Union under the European Social Fund. S.H. acknowledges the

support from the State of Bavaria in Germany. Numerical calculations have been carried out using resources provided by Wroclaw Centre for Networking and Supercomputing [46], Grant No. 203. We are grateful to Krzysztof Gawarecki for sharing his implementation of the $\boldsymbol{k} \cdot \boldsymbol{p}$ method, and Paweł Machnikowski for helpful discussions.

[1] J. Brault, M. Gendry, G. Grenet, G. Hollinger, Y. Desières, and T. Benyattou, Role of buffer surface morphology and alloying effects on the properties of InAs nanostructures grown on InP (001), Appl. Phys. Lett. **73**, 2932 (1998).

[2] A. Sauerwald, T. Kümmell, G. Bacher, A. Somers, R. Schwertberger, J. P. Reithmaier, and A. Forchel, Size control of InAs quantum dashes, Appl. Phys. Lett. **86**, 253112 (2005).

[3] H. Dery, E. Benisty, A. Epstein, R. Alizon, V. Mikhelashvili, G. Eisenstein, R. Schwertberger, D. Gold, J. P. Reithmaier, and A. Forchel, On the nature of quantum dash structures, J. Appl. Phys. **95**, 6103 (2004).

[4] M. Z. M. Khan, T. K. Ng, and B. S. Ooi, Self-assembled InAs/InP quantum dots and quantum dashes: Material structures and devices, Prog. Quantum Electron. **38**, 237 (2014).

[5] K. Ryczko, G. Sęk, and J. Misiewicz, The effect of structural parameters on the in-plane coupling between quantum dashes of a dense ensemble in the InAs-InP material system, J. Appl. Phys. **115**, 213502 (2014).

[6] M. Gawełczyk, M. Syperek, A. Maryński, P. Mrowiński, L. Dusanowski, K. Gawarecki, J. Misiewicz, A. Somers, J. P. Reithmaier, S. Höfling, and G. Sęk, Exciton lifetime and emission polarization dispersion in strongly in-plane asymmetric nanostructures, Phys. Rev. B **96**, 245425 (2017).

[7] J. P. Reithmaier, A. Somers, S. Deubert, R. Schwertberger, W. Kaiser, A. Forchel, M. Calligaro, P. Resneau, O. Parillaud, S. Bansropun, M. Krakowski, R. Alizon, D. Hadass, A. Bilenca, H. Dery, V. Mikhelashvili, G. Eisenstein, M. Gioannini, I. Montrosset, T. W. Berg *et al.*, InP based lasers and optical amplifiers with wire-/dot-like active regions, J. Phys. D **38**, 2088 (2005).

[8] A. Capua, O. Karni, G. Eisenstein, J. P. Reithmaier, and K. Yvind, Extreme nonlinearities in InAs/InP nanowire gain media: The two-photon induced laser, Opt. Express **20**, 5987 (2012).

[9] M. Syperek, L. Dusanowski, J. Andrzejewski, W. Rudno-Rudziński, G. Sęk, J. Misiewicz, and F. Lelarge, Carrier relaxation dynamics in InAs/GaInAsP/InP(001) quantum dashes emitting near 1.55 μm, Appl. Phys. Lett. **103**, 083104 (2013).

[10] G. Sęk, P. Podemski, A. Musiał, J. Misiewicz, S. Hein, S. Höfling, and A. Forchel, Exciton and biexciton emission from a single InAs/InP quantum dash, J. Appl. Phys. **105**, 086104 (2009).

[11] Ł. Dusanowski, M. Syperek, W. Rudno-Rudziński, P. Mrowiński, G. Sęk, J. Misiewicz, A. Somers, J. P. Reithmaier, S. Höfling, and A. Forchel, Exciton and biexciton dynamics in single self-assembled InAs/InGaAlAs/InP quantum dash emitting near 1.55 μm, Appl. Phys. Lett. **103**, 253113 (2013).

[12] Ł. Dusanowski, M. Syperek, J. Misiewicz, A. Somers, S. Höfling, M. Kamp, J. P. Reithmaier, and G. Sęk, Single-photon emission of InAs/InP quantum dashes at 1.55 μm and temperatures up to 80 K, Appl. Phys. Lett. **108**, 163108 (2016).

[13] Ł. Dusanowski, M. Gawełczyk, J. Misiewicz, S. Höfling, J. P. Reithmaier, and G. Sęk, Strongly temperature-dependent recombination kinetics of a negatively charged exciton in asymmetric quantum dots at 1.55 μm, Appl. Phys. Lett. **113**, 043103 (2018).

[14] S. Hein, A. Somers, W. Kaiser, S. Höfling, J. Reithmaier, and A. Forchel, Singlemode InAs/InP quantum dash distributed feedback lasers emitting in 1.9 μm range, Electron. Lett. **44**, 527 (2008).

[15] A. Capua, G. Eisenstein, and J. P. Reithmaier, A nearly instantaneous gain response in quantum dash based optical amplifiers, Appl. Phys. Lett. **97**, 131108 (2010).

[16] A. Capua, O. Karni, G. Eisenstein, and J. P. Reithmaier, Rabi oscillations in a room-temperature quantum dash semiconductor optical amplifier, Phys. Rev. B **90**, 045305 (2014).

[17] Ł. Dusanowski, M. Syperek, P. Mrowiński, W. Rudno-Rudziński, J. Misiewicz, A. Somers, S. Höfling, M. Kamp, J. P. Reithmaier, and G. Sęk, Single photon emission at 1.55 μm from charged and neutral exciton confined in a single quantum dash, Appl. Phys. Lett. **105**, 021909 (2014).

[18] X. Liu, N. Ha, H. Nakajima, T. Mano, T. Kuroda, B. Urbaszek, H. Kumano, I. Suemune, Y. Sakuma, and K. Sakoda, Vanishing fine-structure splittings in telecommunication-wavelength quantum dots grown on (111)A surfaces by droplet epitaxy, Phys. Rev. B **90**, 081301(R) (2014).

[19] N. Ha, T. Mano, T. Kuroda, K. Mitsuishi, A. Ohtake, A. Castellano, S. Sanguinetti, T. Noda, Y. Sakuma, and K. Sakoda, Droplet epitaxy growth of telecom InAs quantum dots on metamorphic InAlAs/GaAs(111)A, Jpn. J. Appl. Phys. **54**, 04DH07 (2015).

[20] N. Ha, T. Mano, Y.-N. Wu, Y.-W. Ou, S.-J. Cheng, Y. Sakuma, K. Sakoda, and T. Kuroda, Wavelength extension beyond 1.5 μm in symmetric InAs quantum dots grown on InP(111)A using droplet epitaxy, Appl. Phys. Express **9**, 101201 (2016).

[21] J. Skiba-Szymanska, R. M. Stevenson, C. Varnava, M. Felle, J. Huwer, T. Müller, A. J. Bennett, J. P. Lee, I. Farrer, A. B. Krysa, P. Spencer, L. E. Goff, D. A. Ritchie, J. Heffernan, and A. J. Shields, Universal Growth Scheme for Quantum Dots with Low Fine-Structure Splitting at Various Emission Wavelengths, Phys. Rev. Appl. **8**, 014013 (2017).

[22] P. Mrowiński, A. Musiał, A. Maryński, M. Syperek, J. Misiewicz, A. Somers, J. P. Reithmaier, S. Höfling, and G. Sęk, Magnetic field control of the neutral and charged exciton fine structure in single quantum dashes emitting at 1.55 μm, Appl. Phys. Lett. **106**, 053114 (2015).

[23] A. Musiał, P. Kaczmarkiewicz, G. Sęk, P. Podemski, P. Machnikowski, J. Misiewicz, S. Hein, S. Höfling, and A. Forchel, Carrier trapping and luminescence polarization in quantum dashes, Phys. Rev. B **85**, 035314 (2012).

[24] Ł. Dusanowski, P. Mrowiński, M. Syperek, J. Misiewicz, A. Somers, S. Höfling, J. P. Reithmaier, and G. Sęk, Confinement regime in self-assembled InAs/InAlGaAs/InP quantum dashes determined from exciton and biexciton recombination kinetics, Appl. Phys. Lett. **111**, 253106 (2017).

[25] M. Gawełczyk, Excitons in asymmetric nanostructures: Confinement regime, Acta Phys. Pol. A **134**, 930 (2018).

[26] M. Holtkemper, D. E. Reiter, and T. Kuhn, Influence of the quantum dot geometry on *p*-shell transitions in differently charged quantum dots, Phys. Rev. B **97**, 075308 (2018).

[27] M. Zieliński, From quantum dots to quantum dashes: Excitonic spectra of highly elongated InAs/InP nanostructures, Phys. Rev. B **99**, 205402 (2019).

[28] A. Maryński, G. Sęk, A. Musiał, J. Andrzejewski, J. Misiewicz, C. Gilfert, J. P. Reithmaier, A. Capua, O. Karni, D. Gready, G. Eisenstein, G. Atiya, W. D. Kaplan, and S. Kölling, Electronic structure, morphology and emission polarization of enhanced symmetry InAs quantum-dot-like structures grown on InP substrates by molecular beam epitaxy, J. Appl. Phys. **114**, 094306 (2013).

[29] W. Rudno-Rudziński, R. Kudrawiec, P. Podemski, G. Sęk, J. Misiewicz, A. Somers, R. Schwertberger, J. P. Reithmaier, and A. Forchel, Photoreflectance-probed excited states in InAs/InGaAlAs quantum dashes grown on InP substrate, Appl. Phys. Lett. **89**, 031908 (2006).

[30] Ł. Dusanowski, P. Holewa, A. Maryński, A. Musiał, T. Heuser, N. Srocka, D. Quandt, A. Strittmatter, S. Rodt, J. Misiewicz, S. Reitzenstein, and G. Sęk, Triggered high-purity telecom-wavelength single-photon generation from p-shell-driven InGaAs/GaAs quantum dot, Opt. Express **25**, 31122 (2017).

[31] P. Podemski, A. Maryński, P. Wyborski, A. Bercha, W. Trzeciakowski, and G. Sęk, Single dot photoluminescence excitation spectroscopy in the telecommunication spectral range, J. Lumin. **212**, 300 (2019).

[32] F. Intonti, V. Emiliani, C. Lienau, T. Elsaesser, R. Nötzel, and K. H. Ploog, Near-field optical spectroscopy of localized and delocalized excitons in a single GaAs quantum wire, Phys. Rev. B **63**, 075313 (2001).

[33] P. Mrowiński, M. Zieliński, M. Świderski, J. Misiewicz, A. Somers, J. P. Reithmaier, S. Höfling, and G. Sęk, Excitonic fine structure and binding energies of excitonic complexes in single InAs quantum dashes, Phys. Rev. B **94**, 115434 (2016).

[34] See Supplemental Material at http://link.aps.org/supplemental/10.1103/PhysRevB.100.241304 for a detailed analysis of the excitation-power dependence of selected emission lines as well as more examples of μPLE traces reproduced within the theoretical model, which includes Refs. [35–37]].

[35] G. Sęk, A. Musiał, P. Podemski, and J. Misiewicz, On the applicability of a few level rate equation model to the determination of exciton versus biexciton kinetics in quasi-zero-dimensional structures, J. Appl. Phys. **108**, 033507 (2010).

[36] M. Grundmann and D. Bimberg, Theory of random population for quantum dots, Phys. Rev. B **55**, 9740 (1997).

[37] M. Abbarchi, C. Mastrandrea, T. Kuroda, T. Mano, A. Vinattieri, K. Sakoda, and M. Gurioli, Poissonian statistics of excitonic complexes in quantum dots, J. Appl. Phys. **106**, 053504 (2009).

[38] A. Lemaître, A. D. Ashmore, J. J. Finley, D. J. Mowbray, M. S. Skolnick, M. Hopkinson, and T. F. Krauss, Enhanced phonon-assisted absorption in single InAs/GaAs quantum dots, Phys. Rev. B **63**, 161309(R) (2001).

[39] T. B. Bahder, Eight-band $\mathbf{k}\cdot\mathbf{p}$ model of strained zinc-blende crystals, Phys. Rev. B **41**, 11992 (1990).

[40] M. G. Burt, The justification for applying the effective-mass approximation to microstructures, J. Phys.: Condens. Matter **4**, 6651 (1992).

[41] B. A. Foreman, Effective-mass Hamiltonian and boundary conditions for the valence bands of semiconductor microstructures, Phys. Rev. B **48**, 4964 (1993).

[42] K. Gawarecki, P. Machnikowski, and T. Kuhn, Electron states in a double quantum dot with broken axial symmetry, Phys. Rev. B **90**, 085437 (2014).

[43] J. Andrzejewski, G. Sęk, E. O'Reilly, A. Fiore, and J. Misiewicz, Eight-band $\mathbf{k}\cdot\mathbf{p}$ calculations of the composition contrast effect on the linear polarization properties of columnar quantum dots, J. Appl. Phys. **107**, 073509 (2010).

[44] Ł. Dusanowski, A. Musiał, A. Maryński, P. Mrowiński, J. Andrzejewski, P. Machnikowski, J. Misiewicz, A. Somers, S. Höfling, J. P. Reithmaier, and G. Sęk, Phonon-assisted radiative recombination of excitons confined in strongly anisotropic nanostructures, Phys. Rev. B **90**, 125424 (2014).

[45] M. Syperek, Ł. Dusanowski, M. Gawełczyk, G. Sęk, A. Somers, J. P. Reithmaier, S. Höfling, and J. Misiewicz, Exciton spin relaxation in InAs/InGaAlAs/InP(001) quantum dashes emitting near 1.55 μm, Appl. Phys. Lett. **109**, 193108 (2016).

[46] http://wcss.pl.